Journal of Magnetic Resonance 199 (2009) 88–93

Contents lists available at ScienceDirect

Journal of Magnetic Resonance

journal homepage: www.elsevier.com/locate/jmr

Nonuniform sampling and spectral aliasing

Mark W. Maciejewski [a], Harry Z. Qui [a], Iulian Rujan [a], Mehdi Mobli [b], Jeffrey C. Hoch [a,*]

[a] University of Connecticut Health Center, Department of Molecular, Microbial, and Structural Biology, 263 Farmington Ave., Farmington, CT 06030-3305, USA
[b] University of Queensland, Institue for Molecular Bioscience, St. Lucia, Qld 4072, Australia

ARTICLE INFO

Article history:
Received 20 November 2008
Revised 10 April 2009
Available online 16 April 2009

Keywords:
Nonuniform Sampling
Spectral aliasing
Maximum entropy reconstruction

ABSTRACT

The Nyquist theorem stipulates the largest sampling interval sufficient to avoid aliasing is the reciprocal of the spectral bandwidth. When data are not sampled uniformly, the Nyquist theorem no longer applies, and aliasing phenomena become more complex. For samples selected from an evenly spaced grid, signals that are *within* the nominal bandwidth of the grid can give rise to aliases. The effective bandwidth afforded by a set of nonuniformly sampled evolution times does not necessarily correspond to spacing of the grid from which the samples are selected, but instead depends on the actual distribution of sample times. For conventional uniform sampling there is no distinction between the grid spacing and the sampling interval. For nonuniform sampling, an effective bandwidth can be inferred from the greatest common divisor of the sample times, provided that none of the sample times are irrational. A simple way to increase the effective bandwidth for a set of nonuniformly spaced samples is to randomly select them from an oversampled grid. For a given grid spacing, "bursty" sampling helps to minimize aliasing artifacts. We show that some spectral artifacts arising from nonuniform sampling are aliases, and that increasing the effective bandwidth shifts these artifacts out of the spectral window and improves spectral quality. An advantage of nonuniform sampling is that some of the benefits of oversampling can be realized without incurring experiment time or resolution penalties. We illustrate the improvements that can be obtained with nonuniform sampling in the indirect dimension of a SOFAST–HMQC experiment.

1. Introduction

The manifestation of spectral aliasing when a time-varying signal is sampled less frequently than stipulated by the Nyquist theorem [1] is straightforward: exact replicas of the signals appear reflected about the limits of the effective bandwidth, a phenomenon commonly referred to as spectral aliasing. The precise frequencies of the aliases depend on the scheme used to discriminate positive and negative frequencies (e.g., the type of quadrature detection). When data is not sampled at uniformly spaced intervals, however, the Nyquist theorem no longer holds. A fundamental question then arises: Can a bandwidth be associated with a set of nonuniformly spaced sampling times? If not, what are the factors that determine whether a spectral component is aliased, and how is aliasing manifested? In this work we demonstrate that in the context of nonuniform sampling (NUS) in the time domain aliasing is not as simple as for uniform sampling, and examine the factors that influence aliasing. For NUS, the spacing of the grid from which samples are selected is not sufficient to define the bandwidth: inadvertent choice of sample times can lead to undersampling. Furthermore, completely random selection (i.e., off-grid) of sample times does not afford infinite bandwidth. These results lead to a simple strategy for reducing artifacts in spectra computed from NUS data. We illustrate the improvements that can be achieved for a NUS SOFAST–HMQC experiment.

2. Spectral estimates for NUS data

With the recent explosion in approaches to fast or sparse data collection in multidimensional NMR, it bears pointing out some distinctions and similarities between different approaches used to compute frequency spectra from NUS data. Methods such as back projection reconstruction (BPR) [2] and G-matrix Fourier transform (GFT) [3] exploit a very specific approach to selecting NUS times, namely coupled evolution periods that result in sampling along radial vectors in the time dimensions. Alternatives to BPR and GFT include "nonuniform Fourier transform" (nuDFT) [4], multidimensional decomposition (MDD) [5], maximum likelihood (MLM) [6] and Bayesian methods [7], and maximum entropy (MaxEnt) [8,9] and forward MaxEnt (FM) [10]. These latter methods are all capable of treating NUS data collected using essentially arbitrary evolution times. Each has strengths and weaknesses; in general, they employ a continuum of assumptions about the data. For example, nuDFT implicitly assumes that times not sampled have zero intensity, and so when samples are selected from a regular grid, the fast Fourier transform (FFT) can be used to compute the nuDFT by setting the data at times not sampled to zero.

* Corresponding author. Fax: +1 860 679 3408.
E-mail address: hoch@uchc.edu (J.C. Hoch).

1090-7807/$ - see front matter © 2009 Elsevier Inc. All rights reserved.
doi:10.1016/j.jmr.2009.04.006

Although nuDFT is numerically efficient, the resulting spectral estimate is a convolution of the point spread function (PSF) for the set of sampled times with the spectrum of the sample [9]. The PSF is obtained from the Fourier transform of a sampling function having the value one for the times sampled and zero for times not sampled. A consequence of this convolution is that sampling artifacts are quite prominent in nuDFT spectra, and nuDFT spectra frequently need post-processing to deconvolve the PSF in order to be useful.

MLM and Bayesian methods both assume a model for the signals, usually treating the signal as a sum of exponentially decaying sinusoids. As parametric methods of signal processing they can be quite powerful when the assumption of exponential decay is valid and the number of sinusoids is not underestimated. When either of these conditions is violated, however, substantial bias can result. Because all signal components including noise are modeled as exponentially decaying sinusoids, these methods are prone to false positives. MDD makes a less restrictive assumption that the multidimensional spectrum (or signal) can be decomposed into a small set of one-dimensional vectors; the multidimensional spectrum is given by the vector outer product of the one-dimensional vectors. MDD requires three- or higher-dimensional data, and thus is not applicable to two-dimensional experiments. One aspect of MDD that remains under-investigated is the response to noise: it is axiomatic that uncorrelated noise cannot be decomposed into a vector product, and the manifestations of noise in MDD spectra and the threshold at which MDD breaks down are not well understood. The assumption underlying MDD is more general than that employed by MLM or Bayesian approaches, however, as it is applicable in principle to arbitrary lineshapes, i.e., signals exhibiting nonexponential decay.

MaxEnt is perhaps the most general of the methods suitable for NUS data, as it assumes only that the noise is randomly distributed. In the absence of empirical evidence MaxEnt biases the spectrum toward zero; FM is related to more general MaxEnt by using the maximum entropy principal to estimate values for samples not collected in the NUS set, while enforcing an exact match between the inverse DFT of the spectral estimate with the samples in the NUS set. FM is thus equivalent to MaxEnt reconstruction in the limit of infinite weight on the constraint enforcing agreement between the inverse DFT of the reconstructed spectrum and the measured data; in essence, the entropy is used to interpolate the data for times not sampled.

3. nuDFT: a misnomer

Although the discrete Fourier transform can be modified to accommodate arbitrary sample times, when used with nonuniformly spaced samples it no longer corresponds to an expansion in an orthonormal Fourier basis set and is thus not strictly speaking a transform. The non-orthogonality of the basis functions over a set of nonuniform sample times, even if they are selected from a uniform grid, results in interference between signal components and is one perspective from which to view sampling artifacts. The use of weights can in some circumstances improve the accuracy of nuDFT, as is frequently employed in the realm of numerical quadrature on an irregular mesh. The appropriate weights correspond to the Jacobian (ratio of partial derivatives) used when changing variables under an integral, as employed by Coggins and Zhou in their demonstration of the equivalence between back projection and radial Fourier Transformation [11]. In the discrete case, or when the sampling scheme lacks an analytic description, the appropriate weights are given by the Voronoi area or volume (for 2D or 3D nonuniform sampling, respectively) around each sample time, as shown by Pannetier et al. [12] Despite the limitations of nuDFT, it yields a linear spectral estimate and places useful bounds on the sampling artifacts that nonlinear methods help to reduce. Here we use unweighted nuDFT to explore aliasing artifacts due to NUS.

4. Aliasing with NUS: imperfect aliasing

With uniform sampling, signal components with frequencies higher than the reciprocal of the sampling interval are "perfectly" aliased, that is they appear at a lower frequency but the *same* amplitude as in a non-aliased spectrum (i.e., one obtained with a higher sampling rate, Fig. 1) [1]. When the same signal is sampled nonuniformly by selecting a subset of the sample values, artifacts appear at the same locations as before, but with *different* amplitudes. The alias and the original peak are both broadened, in the nuDFT spectrum, by an amount corresponding to the width of the zero-frequency component of the PSF. The magnitude of the artifacts depends on the frequencies of the signal components and the distribution of sample times in the subset. We refer to aliases resulting from signals with frequencies that exceed the reciprocal of the grid spacing as extra-band aliases. Those arising from signals that do not exceed the reciprocal of the grid spacing we refer to as intra-band aliases; these aliases are not present in spectra of uniformly sampled data.

Fig. 2 depicts example spectra for a noiseless, synthetic signal sampled nonuniformly and computed using nuDFT. We conducted a more systematic computer experiment in which 10000 randomly generated NUS schedules were used to sample 20 different synthetic data sets, each containing a single randomly selected frequency component. Fig. 3 shows the amplitudes of the intra-band aliases (relative to the non-aliased peak) averaged over the 20 spectra, as a function of the average sampling rate, defined as the average of the reciprocal of the time interval between successive samples for each of the 10000 randomly generated nonuniform sampling schedules. The average sampling rate is reported as a unitless fraction of the rate of sampling on the uniform grid; a schedule that utilizes alternate points on the grid would have an average sampling rate of 0.5, while uniform sampling of the first 50% of the points on the grid would have an average rate of 1.0. Each sampling schedule consists of 32 sample times selected from a uniform 64-element grid. The 10 sampling schedules that on average lead to the smallest intra-band aliases (values near 0.01 in panel A) and the 10 that lead to the largest intra-band aliases (near the top of the distribution in panel A) are depicted in panels B and C, respectively. The best schedules (panel B) qualitatively appear to be more "bursty" than the worst schedules. Although burst sampling is routinely used in frequency estimation [13] and "burstiness" is an important characteristic of network traffic, there is no established metric for quantifying "burstiness". We plan to explore this issue further.

Comparison of a nuDFT spectrum with a spectrum computed using a method that deconvolves sampling artifacts (such as MaxEnt) reveals another distinction between intra-band aliases and extra-band aliases. Fig. 4 compares spectra obtained from a synthetic signal containing two signal components, sampled from a grid corresponding to a 10,000 Hz bandwidth. One component has a frequency of 1500 Hz (as in Fig. 2) and the other has a frequency of 8000 Hz, outside the nominal bandwidth (±5000 Hz) of the grid. Panel A depicts the DFT of the uniformly sampled data, with the extra-band alias peak indicated by an asterisk. Panels B and C depict the nuDFT and MaxEnt reconstructions (computed using the Rowland NMR Toolkit [14]), respectively, using the nonuniform sampling schedule depicted in panel D. Intra-band aliases appear in B and C are indicated by diamonds. In the MaxEnt spectrum the intra-band aliases are diminished, but the extra-band

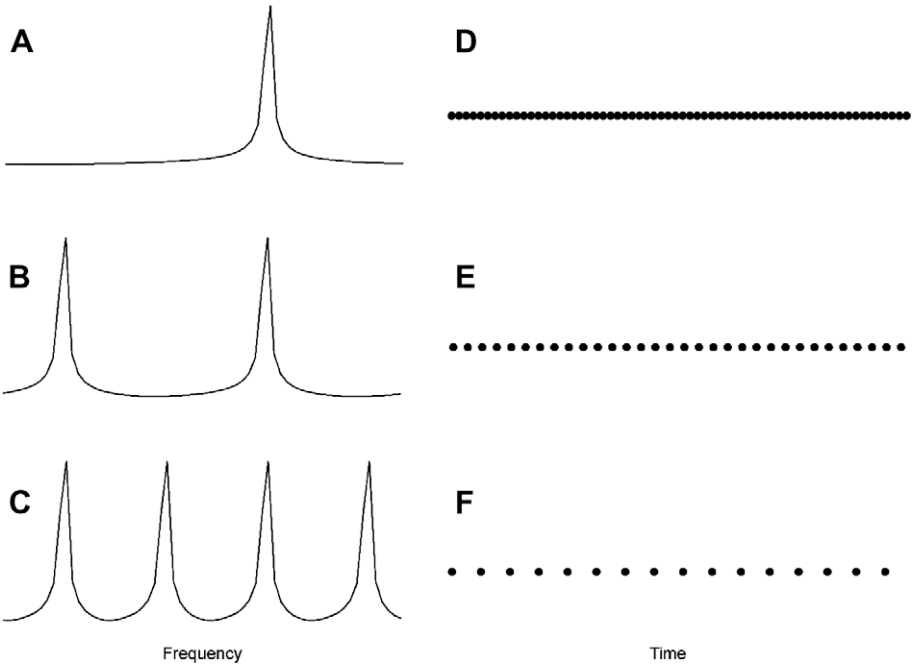

Fig. 1. Examples of aliasing using uniform sampling. Each panel depicts a uniform sampling scheme above the DFT spectrum for a single synthetic sinusoid. (A) Uniform sampling at the Nyquist rate. (B) Uniform sampling at one-half the Nyquist rate. (C) Uniform sampling at one-quarter the Nyquist rate. (D, E and F) Depict the sampled times for A, B and C, respectively.

alias remains unaffected. In the MaxEnt spectrum of this noiseless synthetic data, the parameter "aim" that corresponds to the experimental uncertainty is set to an arbitrary value (aim is the root-mean-square difference between the measured data and the "mock data" obtained by inverse FT of the MaxEnt spectrum; it normally is set to a value comparable but somewhat larger than the estimated noise level. Here it need only be set to a value smaller than the total power in the noiseless signal). In principle it could be set to an extremely small value that would lead to complete deconvolution of the sampling artifacts (including the NUS alias peak), but such perfect deconvolution is never achievable for real data containing noise.

5. On vs. off-grid sampling

If NUS is not restricted to a subset of samples from the Nyquist grid (the grid with times spaced at the Nyquist interval), it is not obvious whether or where to expect aliases. As pointed out by Bretthorst [15,16], any set of arbitrary sample times can be placed on a uniform grid so long as the sample times have finite precision (i.e., the times are not irrational). The grid is specified by the least significant digit in the sample times (determined by the precision of the spectrometer timing circuitry). The least significant digit is actually a lower bound on the grid spacing, as there may be a common divisor that is larger. The greatest common divisor (GCD) specifies the grid with the largest possible spacing, containing the fewest elements sufficient to accommodate the sample set. The GCD can be computed using a number of different approaches, for example by finding common factors for successive pairs of evolution times or by finding the prime factors for all the evolution times (when converted to integers by shifting the decimal point) and counting the common factors. The reciprocal of the GCD specifies a nominal bandwidth for an off-grid sample set, and is finite. The suggestion that random sampling corresponds to infinite

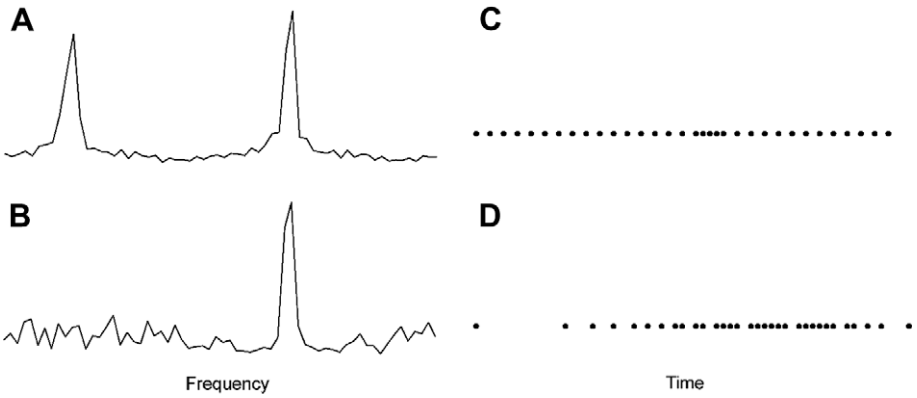

Fig. 2. Imperfect aliasing with nonuniform sampling. The panels on the left (A and B) depict the nuDFT (DFT in which samples not measured are set to zero) for the same synthetic signal as Fig. 1, using nonuniform sampling from the Nyquist grid as depicted in the panels on the right (C and D). (A) An alias appears at the frequency expected using deliberate undersampling by a factor of two, but with a height slightly less than the true (unaliased) peak. (B) The alias is greatly diminished, a result of the greater number of samples in the NUS set spaced at the Nyquist interval.

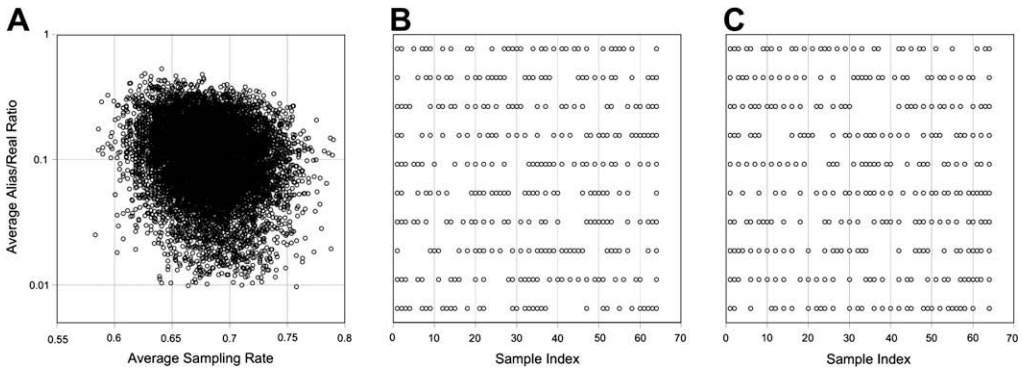

Fig. 3. Results for random sampling schemes. 10,000 schemes were generated by randomly selecting 32 sample times from a uniform grid of 64 samples. (A) Ratio between the alias peak height and the real peak height, averaged over 20 different synthetic data sets, each containing a single randomly selected frequency component, plotted against the average sampling rate in fractional units of the rate corresponding to the uniform grid. The ten best (smallest alias/real ratio) and ten worst (largest alias/real ratio) are depicted (B and C), respectively. The best schedules (B) tend to be "bursty".

bandwidth [17] is only correct if the sample times are specified with infinite precision and the times are relatively prime.

6. Oversampling and randomness to decrease GCD

One way to ensure that a set of NUS times have the smallest feasible GCD is to ensure that they are relatively prime, that is they have no common factor other than "1" in the least significant digit. This can be accomplished by ensuring that the times themselves (scaled to integer values) are prime numbers. A more practical method is to select NUS subsets from an oversampled grid, with a spacing given by an integer fraction of the Nyquist interval for the desired bandwidth. Timing circuits on modern commercial NMR spectrometers typically have nominal timing accuracy of 25 nsec or better, corresponding to a Nyquist grid with a 40-MHz bandwidth. This suggests that oversampling of up to 1000-fold should be feasible for the indirect dimensions of typical biomolecular NMR experiments. While selecting samples from an oversampled grid does not ensure that the GCD or smallest sampling interval will match the grid spacing, by employing some degree of randomness or some other irregular scheme for selecting the NUS subset, there is a reasonably high likelihood of obtaining a set with a GCD equal to the grid spacing. For very small subsets of a grid, however, substantial aliasing of peaks within the nominal bandwidth of the grid is unavoidable.

7. Results and discussion: application to SOFAST–HMQC

To illustrate the advantages of decreasing the GCD for a NUS set, we applied NUS to a SOFAST–HMQC experiment [18]. SOFAST experiments exploit the concept of the Ernst angle [19] to optimize sensitivity for a given relaxation delay between FIDs, and are particularly useful in applications to labile systems (for example measuring H-exchange rates). NUS enables a reduction in the number of samples required to collect data at long evolution times necessary for high resolution, thus enabling additional time savings

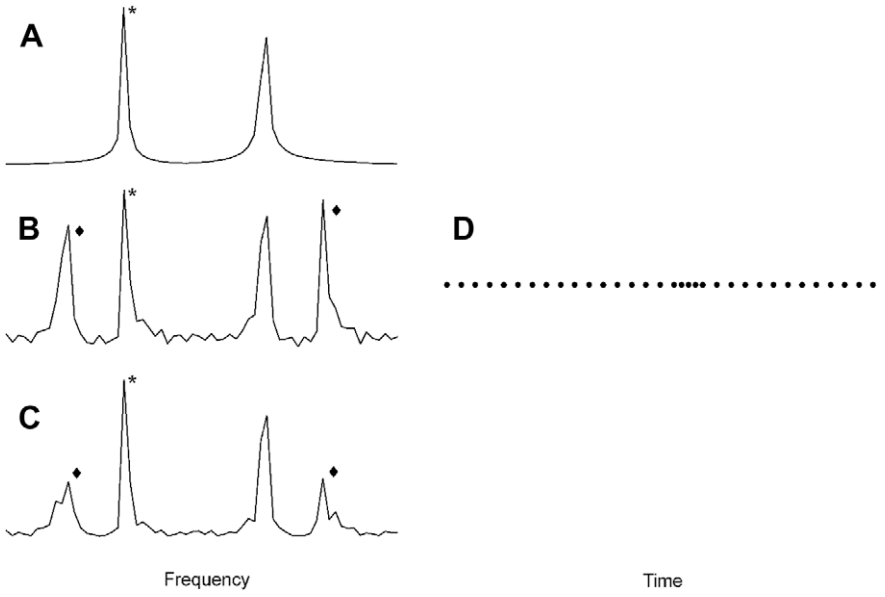

Fig. 4. MaxEnt reconstruction diminishes sampling-related (intra-band) aliases. Top spectrum: DFT spectrum of a uniformly sampled synthetic signal containing two frequency components, one within the Nyquist bandwidth (appear on the right of the spectrum) and one outside the Nyquist bandwidth (on the left). Middle spectrum: nuDFT of NUS data for the same signal, sampled as depicted below the spectrum. Bottom spectrum: MaxEnt reconstruction of the same NUS data; only the NUS-related aliases are diminished. Asterisks denote extra-band aliases. Diamonds denote intra-band aliases.

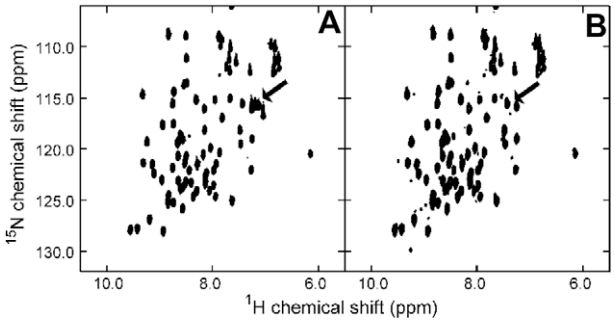

Fig. 5. Conventional (DFT) SOFAST–HMQC spectra for ubiquitin, uniformly sampled in t_1 at rates corresponding to 1600 Hz (A) and 6400 Hz (B). Signals indicated by the arrow are from Arg residues that resonate outside the 1600 Hz bandwidth.

and extending the range of rates accessible by SOFAST experiments. MaxEnt reconstruction is an apt choice for computing the spectrum, because the experiment is two-dimensional, and approaches such as MWD are thus not applicable.

For reference, conventional DFT SOFAST–HMQC spectra for ubiquitin computed from uniformly sampled data are shown in Fig. 5. Panel A shows the spectrum computed from data sampled at a rate corresponding to a 1600 Hz bandwidth; panel B shows the spectrum computed from data sampled at a rate 4 times higher. The arrows in both panels illustrate the position of side chain Arg peaks that resonate near 71 ppm (^{15}N) that are aliased into the spectrum in panel A. Fig. 6 illustrates MaxEnt spectra of NUS SOFAST–HMQC data with NUS applied along the indirect time dimension. Panel A employed 77 samples out of a 256-point 1600 Hz bandwidth grid, while Panels B and C employed 77 samples out of a 1024-point (4× oversampled) grid and a 4096-point (8× oversampled) grid, respectively. The top row depicts one-dimensional cross-sections through the spectra at the frequency indicated by the red line in Panels A–C. The sampled times are very similar for all three experiments, selected randomly from a decaying exponential distribution corresponding to a 12.5 Hz line width and each having approximately the same maximum evolution time. Each experiment results in a better than 3-fold reduction in experiment time compared to uniform sampling. The aliased Arg peaks in panel A (near 7 ppm in the ^{1}H trace) are clearly eliminated in panels B and C. Noise levels in the spectra are improved by selecting the NUS from oversampled grid, a result of shifting some sampling artifacts out of the 10000-Hz spectral window. This effect is explained by the PSFs for the NUS sets, shown in Fig. 7. Some of the sampling noise apparent with sampling on the Nyquist (1×) grid results from aliasing, so oversampling shifts this noise out of the spectral region of interest. The central or zero-frequency component of the PSF becomes broader as the grid spacing is decreased. No attempt to deconvolve additional signal decay was employed in the MaxEnt computations shown in Fig. 6, and in principle the broadening effects of NUS on an oversampled grid could be reduced by deconvolution. The GCD for the NUS sets for the three sampling schemes are 1/1600, 1/6400, and 1/12800 s, each matching the spacing of the underlying grids.

In addition to reducing sampling noise, comparison of Figs. 5 and 6 illustrates that NUS from an oversampled grid coupled with MaxEnt reconstruction (or other methods capable of processing NUS data) affords the anti-aliasing benefits of oversampling without incurring the multiplicative time cost that would be associated with uniform oversampling and conventional (DFT) processing. Improvements in sensitivity that can be obtained through uniform oversampling, provided that the majority of additional samples collected as a result of oversampling correspond to evolution times less than $1.5T_{2*}$ [20], will in general not be obtained by NUS oversampling, however.

8. Concluding remarks

The influence of the NUS strategy on aliasing is another illustration that the most important determinant of the quality of NUS spectral quality is the choice of sampled times. With the exception of nuDFT, all existing methods for spectral estimation from NUS data attempt to deconvolve the PSF from the spectrum to some degree. The frequency dependence of aliasing when NUS is employed is more complex than that for uniform sampling, and the Nyquist theorem no longer applies. The GCD is the determinant of aliasing effects with NUS. The use of an oversampled grid and random sampling to select NUS sets is a simple method for decreasing the GCD and thus shifting aliased noise—both sampling and experimental—out of the spectral region of interest. An advantage of the GCD as a metric for the effective bandwidth is that it is applicable to on or off-grid sampling schemes, provided that the off-grid times are specified with finite precision. However, the complexity of aliasing when NUS is employed necessitates additional metrics, such as the fraction of samples separated by the GCD. The decrease in

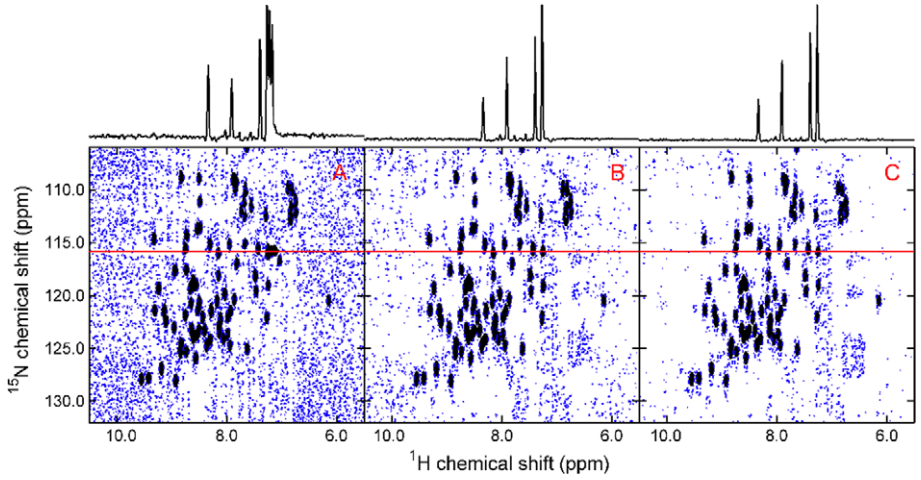

Fig. 6. MaxEnt NUS SOFAST–HMQC spectra for ubiquitin, using t_1 samples selected using a decaying exponential density function corresponding to a 12.5 Hz linewidth. Left: 77 samples from a 256-point 1× (1600 Hz) grid. Middle: 77 samples from a 1024-point 4× (6400 Hz) grid. Right: 77 samples from a 2048-point 8× (12800 Hz) grid. One-dimensional cross-sections taken at the position of the horizontal line near 116 ppm (^{15}N) are plotted above each contour plot.

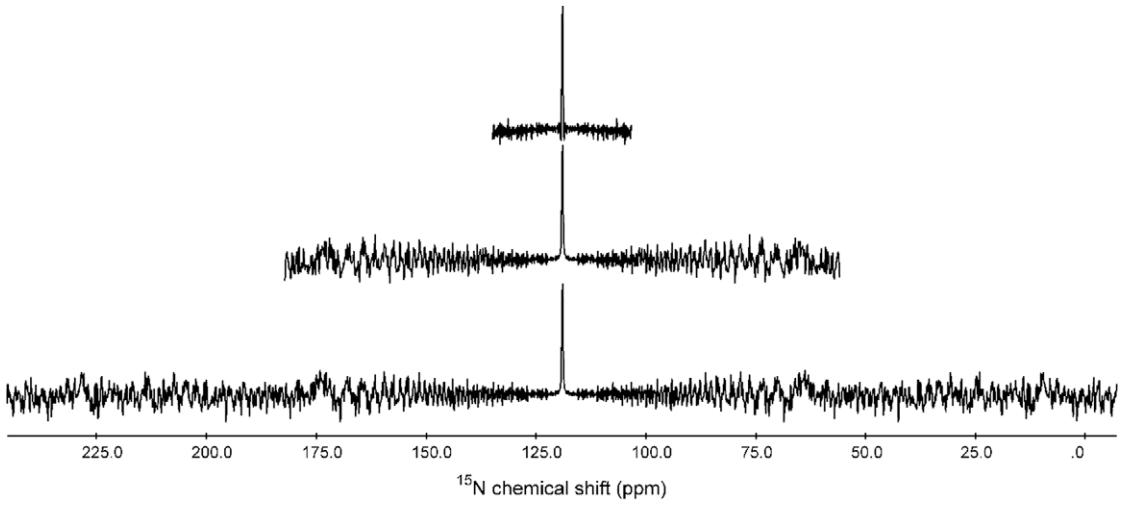

Fig. 7. PSFs for the three NUS schedules used in Fig. 6, corresponding to Nyquist rate, or 1× (top), 4× (middle), and 8× (bottom) oversampling.

sampling artifacts afforded by decreasing the GCD or selecting samples from an oversampled grid effectively increases the effective dynamic range of NUS. Oversampling has previously been shown to improve dynamic range for uniformly sampled data [21,22], and the reduction of sampling artifacts in the spectral region of interest provides additional incentive for employing oversampling in the design of NUS experiments. The results demonstrated here for NUS applied to one indirect dimension should be achievable in all indirect dimensions of multidimensional experiments, and in principle the benefits (e.g., noise reduction) should be multiplicative. We are actively exploring the achievable gains for two and three indirect dimensions.

For the practicing NMR spectroscopist, the fundamental question about NUS is what is the optimal sampling scheme? While we have learned a great deal about how to improve sensitivity and resolution and minimize artifacts, we still do not know how to determine if a sampling scheme is optimal. One reason defining an optimal schedule is so difficult is that "optimality" depends on the frequency distribution of the signals. Another is that there is no consensus on metrics for sensitivity or resolution. Critical comparison of different approaches—either for NUS schemes or spectral reconstruction methods for NUS data—is hampered by this lack of consensus, and the lack of standard test data. Recent initiatives toward collaborative efforts to address these stumbling blocks, such as a workshop at the 49th Experimental NMR Conference, should begin to bear fruit in the near future.

Acknowledgments

This work has been supported by grants from the US National Institutes of Health (RR020125, GM47467, GM072000). We thank Dr. Alan Stern for useful discussions.

References

[1] E.O. Brigham, The Fast Fourier Transform, Prentice-Hall, Inc., Englewood Cliffs, New Jersey, 1974.
[2] E. Kupce, R. Freeman, Projection–reconstruction of three-dimensional NMR spectra, J. Am. Chem. Soc. 125 (2003) 13958–13959.
[3] S. Kim, T. Szyperski, GFT NMR, a new approach to rapidly obtain precise high-dimensional NMR spectral information, J. Amer. Chem. Soc. 125 (2003) 1385–1393.
[4] K. Kazimierczuk, W. Kozminski, I. Zhukov, Two-dimensional Fourier transform of arbitrarily sampled NMR data sets, J. Magn. Reson. 179 (2006) 323–328.
[5] V.Y. Orekhov, I.V. Ibraghimov, M. Billeter, MUNIN: a new approach to multi-dimensional NMR spectra interpretation, J. Biomol. NMR 20 (2001) 49–60.
[6] R.A. Chylla, J.L. Markley, Theory and application of the maximum likelihood principle to NMR parameter estimation of multidimensional NMR data, J. Biomol. NMR 5 (1995) 245–258.
[7] G.L. Bretthorst, Bayesian analysis I. Parameter estimation using quadrature NMR models, J. Magn. Reson. 88 (1990) 533–551.
[8] J.C.J. Barna, E.D. Laue, Conventional and exponential sampling for 2D NMR experiments with application to a 2D NMR spectrum of a protein, J. Magn. Reson. 75 (1987) 384–389.
[9] P. Schmieder, A.S. Stern, G. Wagner, J.C. Hoch, Application of nonlinear sampling schemes to COSY-type spectra, J. Biomol. NMR 3 (1993) 569–576.
[10] S.G. Hyberts, G.J. Heffron, N.G. Tarragona, K. Solanky, K.A. Edmonds, H. Luithardt, J. Fejzo, M. Chorev, H. Aktas, K. Colson, K.H. Falchuk, J.A. Halperin, G. Wagner, Ultrahigh-resolution (1)H–(13)C HSQC spectra of metabolite mixtures using nonlinear sampling and forward maximum entropy reconstruction, J. Am. Chem. Soc. 129 (2007) 5108–5116.
[11] B.E. Coggins, P. Zhou, Polar Fourier transforms of radially sampled NMR data, J. Magn. Reson. 182 (2006) 84–95.
[12] N. Pannetier, K. Houben, L. Blanchard, D. Marion, Optimized 3D NMR sampling for resonance assignment of partially unfolded proteins, J. Magn. Reson. 186 (2007) 142–149.
[13] W.J. Emery, R.E. Thomson, Data Analysis Methods in Physical Oceanography, second and revised ed., Elsevier, 2001.
[14] J.C. Hoch, A.S. Stern, NMR Data Processing, Wiley-Liss, New York, 1996.
[15] G.L. Bretthorst, Nonuniform sampling: bandwidth and aliasing, in: J. Rychert, G. Erickson, C.R. Smith (Eds.), Maximum Entropy and Bayesian Methods in Science and Engineering, Springer, New york, 2001, pp. 1–28.
[16] G.L. Bretthorst, Nonuniform sampling: Bandwidth and aliasing, Concepts Magn. Reson. 32A (2008) 417–435.
[17] K. Kazimierczuk, A. Zawadzka, W. Kozminski, I. Zhukov, Random sampling of evolution time space and Fourier transform processing, J. Biomol. NMR 36 (2006) 157–168.
[18] P. Schanda, B. Brutscher, Very fast two-dimensional NMR spectroscopy for real-time investigation of dynamic events in proteins on the time scale of seconds, J. Am. Chem. Soc. 127 (2005) 8014–8015.
[19] R.R. Ernst, Sensitivity enhancement in magnetic resonance, Adv. Magn. Reson. 2 (1966) 1–135.
[20] D. Rovnyak, J.C. Hoch, A.S. Stern, G. Wagner, Resolution and sensitivity of high field nuclear magnetic resonance spectroscopy, J. Biomol. NMR 30 (2004) 1–10.
[21] R.A. Beckman, E.R.P. Zuiderweg, Guidelines for the use of oversampling in protein NMR, J. Magn. Reson. A113 (1995) 223–231.
[22] M.A. Delsuc, J.Y. Lallemand, Improvement of dynamic range in NMR by oversampling, J. Magn. Reson. 69 (1986) 504–507.